

A Variable Voltage MPPT Control Method for Photovoltaic Generation System

Liu Liqun

Department of Electrical Engineering,
Shanghai Jiaotong University,
Shanghai, 200240, China;

Department of electronic and information
Taiyuan University of Science & Technology,
Taiyuan 030024, Shanxi Province, China
Email: llqd2004@163.com

Wang Zhixin

Department of Electrical Engineering,
Shanghai Jiaotong University,
Shanghai, 200240, China;
wangzxin@sjtu.edu.cn

Abstract: - To increase the output efficiency of a photovoltaic (PV) generation system it is important to have an efficient maximum power point tracking (MPPT) technique. This paper describes the analysis, design and implementation of an efficient tracking method for a stand-alone PV generation system, which automatically adjusts the reference of output voltage to track the maximum power point (MPP) by using the expiatory program. Compared with the conventional constant voltage (CV) method, the proposed approach can effectively improve the tracking speed and accuracy simultaneously. Furthermore, an improved control system is designed for the pulse-width-modulation (PWM) inverter to achieve the objective of MPPT. Theoretical analysis and principle of proposed method are presented and simulation results are given to verify the validity of control method

Key-Words: - Maximum power point tracking (MPPT), Variable voltage, Pulse-width-modulation (PWM), Photovoltaic generation system, Solar energy

1 Introduction

At present, renewable energy sources, i.e., solar energy, wind energy, biomass energy, etc., are regarded for electrical power generate due to their sustainable characteristic and environmental friendly nature [1]. Researches of PV generation systems are actively being regarded to mitigate environment issues such as the green house effect and environment pollution. The conventional PV generation systems have two big problems that the efficiency of PV system is very low, especially under low irradiation states and the output available power of PV system is always changing with weather conditions, i.e., the intensity of the solar radiation (irradiation) and ambient temperature [2-4]. A typical PV installation is composed of: PV panels, regulator, batteries and the inverter. The regulator is the element which is connected between the PV panels and the batteries and its mission is to keep the batteries charged and avoid their overcharge [5]. But a photovoltaic generate system still requires expensive initial investments. In order to extract as much energy as possible from a PV system, it is

important to have an efficient Maximum Power Point Tracking algorithm. In developing nations, the PV generate system is expected to play an important role in total electrical energy demand, and solar photovoltaic energy has gained a lot of attention because it is renewable, friendly to the environment, and flexible for installation. And more and more specialist of China realized the fundamentality of PV generate systems. In order to extract as much energy as possible from a PV system, it is important to have an efficient Maximum Power Point Tracking algorithm.

Various MPPT algorithms and control methods for PV generate system have been described in the literature [1-13], such as a cost-effective single-stage inverter with maximum power point tracking (MPPT) in combination with one-cycle control (OCC) for photovoltaic power generation is proposed in the literature[1]. The linearity method is a novel method in order to track the maximum power point, the proportionality coefficient of the prediction line is automatically corrected using the hill-climbing method when the panel temperature of

the solar arrays is changed [2-4]. The literature [5] presents a regulator which can operate in the maximum power point of PV arrays regardless of the meteorological conditions and the effects of them in the dispersion of the PV array characteristics. A comparative study of the maximum power point trackers using a switching-frequency modulation scheme (SFMS) for photovoltaic panels is presented [6]. Method of locating the maximum power point (MPP) is based on injecting a small-signal sinusoidal perturbation into the switching frequency of the converter and comparing the ac component and the average value of the panel's terminal voltage. The incremental conductance (IC) method is proposed in the literature [7], which is based on the Incremental Conductance method but does not require any current sensing devices. The perturbation and observation (PO) method is well known as the hill-climbing method, it has been widely used because of its simple feedback structure and fewer measured parameters. A digital hill-climbing control strategy combined with a bidirectional current mode power cell is presented which allows getting a regulated bus voltage topology [8]. The constant voltage (CV) and perturbation and observation (PO) method are very common, a cost-effective two-method MPPT control scheme is proposed in this paper to track the maximum power point (MPP) at both low and high irradiation, by combining a Constant Voltage (CV) method and a modified PO algorithm [9]. The fuzzy methods are described in the literature [10-12] that focus on the nonlinear characteristics of PV. A Rapid MPPT Algorithm Based on the Research of Solar Cell's Diode Factor and Reverse Saturation Current are described in the literature [13], which described that how to gain the actual Diode Factor and Reverse Saturation Current of a solar cell and actual Maximum Power Point (MPP), and the output current is controlled in order to track the actual MPP.

Although, various methods of MPPT control have been proposed in existing literature, but the power generate efficiency is relative low, and the amount of electric power generated by solar arrays is always changing with weather conditions. Different solar panel have different diode factor (n) and reverse saturation current (I_0). So they are impossible to quickly acquire the generate power at the maximum power point (MPP). The essential reason is the unknown values of n and I_0 . The theoretical and simulative results show that a piece of PV have same photocurrent under different diode factor n and reverse saturation current I_0 and the weather conditions are sameness conditions. The conclusion

is very important to acquire the actual diode factor and reverse saturation current.

In this paper, first, a piece of PV have same photocurrent under different diode factor n and reverse saturation current I_0 conditions is testified by using the theoretical and simulative results, and the conventional combined perturb and observe (PO) method is used to acquire the actual n and I_0 . Next, the linear relationship between the optimal output voltage and the open-circuit voltage is described in next section. Then, an expiatory program of reference voltage is applied to acquire the actual maximum power point, and a rapid Variable Voltage maximum power point tracking method is described which is based on the actual n and I_0 . Finally, a new proposed double-loop control scheme and the Sepic converter are used to verify the correctness and validity of MPPT algorithm, and the simulation results shows that the proposed MPPT control method improve the tracking speed and accuracy for PV generation system during tracking course.

2 Principle analyzing and modeling of PV

2.1 PV modeling

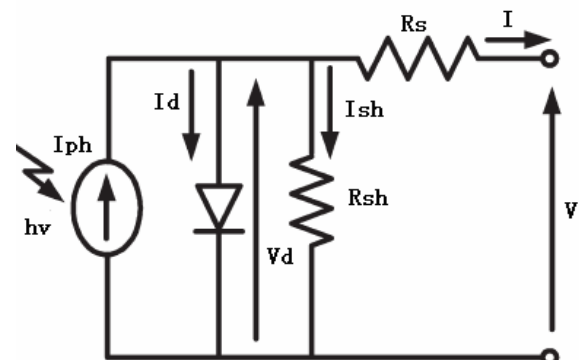


Fig.1, Equivalent circuit for PV

The literature [3-11] proposed various modelling of PV. The output current I and output voltage V of PV is given by (1) and (2) using the symbols in Fig. 1,

$$I = I_{ph} - I_d - V_d / R_{sh} \quad (1)$$

$$V = V_d - R_s I \quad (2)$$

$$I_d = I_0 \left[\exp\left(\frac{qV_d}{nkT}\right) - 1 \right] \quad (3)$$

where I_{ph} is the photocurrent (in amperes), I_0 is the reverse saturation current (in amperes), I_d is the average current through diode (in amperes), n is the diode factor, q is the electron charge (in coulombs), $q = 1.6 \times 10^{-19} C$, k is Boltzmann's constant (in joules per Kelvin), $k = 1.38 \times 10^{-23} J/K$, and T is the PV panel temperature (in Kelvin). R_s

stands for the intrinsic series resistance of the PV, which is ideally zero. R_{sh} denotes the equivalent shunt resistance of the solar array, which is ideally infinity. In general, the output current of PV is expressed by

$$I = I_{ph} - I_0 \left[\exp \left\{ \frac{q}{nkT} (V + R_s I) \right\} - 1 \right] - \frac{V + R_s I}{R_{sh}} \quad (4)$$

Where the resistances R_s and R_{sh} can generally be neglected, and therefore, last term in (4) is generally dropped.

$$I = I_{ph} - I_0 \left[\exp \left\{ \frac{q}{nkT} (V) \right\} - 1 \right] \quad (5)$$

When the circuit is opened, the output current $I = 0$, and the open-circuit voltage V_{oc} is expressed by

$$V_{oc} = V \max = \frac{nkT}{q} \ln \left(\frac{I_{ph}}{I_0} + 1 \right) \approx \frac{nkT}{q} \ln \left(\frac{I_{ph}}{I_0} \right) \quad (6)$$

If the circuit is shorted, the output voltage $V = 0$, the average current through diode I_d is generally be neglected, and the short-circuit current $I_{sc} = I$ is expressed by using (7). The relationship exists between short-circuit current I_{sc} and photocurrent I_{ph} by using (8).

$$I = I_{ph} - \frac{R_s I}{R_{sh}} \quad (7)$$

$$I = I_{sc} = I_{ph} / \left(1 + \frac{R_s}{R_{sh}} \right) \approx I_{ph} \quad (8)$$

Finally, the output power P is expressed by (9)

$$P = IV = (I_{ph} - I_d - V_d / R_{sh})V = (I_{ph} - I_d)V \quad (9)$$

$$= (I_{ph} - I_0 \{ \exp [\frac{q}{nkT} (V)] - 1 \})V$$

$$P_{max} = I_{ph} \left\{ V_{oc} - \frac{nkT}{q} \ln \left(1 + \frac{qV_{mppt}}{nkT} \right) \right\} - \frac{V_{oc}}{qV_{mppt}(nkT)} + \left(\frac{nkT}{q} \right)^2 \frac{1}{V_{mppt}} \ln \left(1 + \frac{qV_{mppt}}{nkT} \right) \quad (10)$$

Here P and V are the instantaneous output power and output voltage of PV, respectively. The steady-state of the maximum power point (MPP) contains $\partial P / \partial V = 0$. The maximum power P_{max} is expressed by (10). Here P_{max} and V_{mppt} are the maximum output power and optimal output voltage at the time, respectively.

$$I_{sc} = I_{sc}(25^\circ C, 1KW/m^2) \times S / 1000 \quad (11)$$

$$I_{ph}(25^\circ C, 1KW/m^2) = I_{sc}(25^\circ C, 1KW/m^2) \quad (12)$$

$$\times (1 + R_s / R_{sh}) \approx I_{sc}(25^\circ C, 1KW/m^2)$$

$$I_{ph} = I_{ph}(25^\circ C, 1KW/m^2) \times [1 + K_i \times (T - T_r)] \quad (13)$$

$$\times (1 + R_s / R_{sh}) \times S_j / 1000$$

$$S = \frac{I_{ph} \times 1000}{I_{ph}(25^\circ C, 1KW/m^2) \times [1 + K_i \times (T - T_r)] \times (1 + R_s / R_{sh})} \quad (14)$$

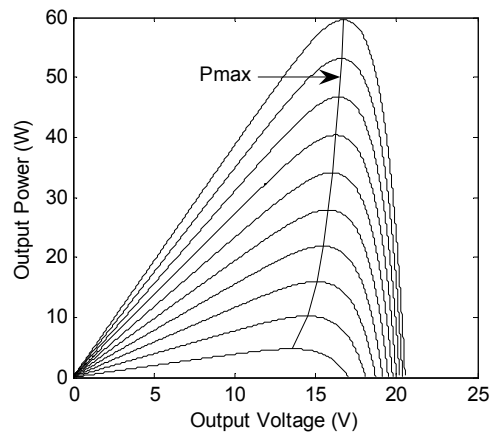
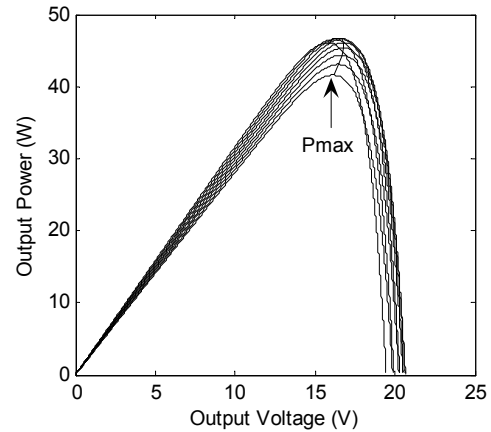


Fig.2 Calculated P-I characteristics and P_{max} curve under the known n and I_0 conditions. (a) The irradiation S is $800W/m^2$, and the temperature is changing from $-50^\circ C$ to $75^\circ C$. (b) The irradiation is changing from $100W/m^2$ to $1KW/m^2$ at the temperature $45^\circ C$.

Many parameters affect the output power of PV generation system, such as two intrinsic resistances, ambient temperature, the solar irradiation, the diode factor and the reverse saturation current. Firstly, R_s is very small ($m\Omega$), and R_{sh} is very large (in $k\Omega$) in actual PV system, and the values of two intrinsic resistances are the unknown constants. Secondly, the output power of PV is affected by the temperature and irradiation. The short-circuit current I_{sc} and the open-circuit voltage V_{oc} of PV are always changing with the ambient temperature and solar irradiation. If the temperature is changeable, the changing coefficient K_v of V_{oc} is $(-0.37 \sim -0.4\%) / ^\circ C$ at solar panel temperature $25^\circ C$, the changing coefficient K_i of I_{sc} is $(+0.09 \sim +0.1\%) / ^\circ C$ at solar panel temperature $25^\circ C$, where, T_r are $25^\circ C$ (in Kelvin). If the irradiation is changeable, the short-circuit current I_{sc} is expressed by using (11) at temperature $25^\circ C$. Here $I_{sc}(25^\circ C, 1KW/m^2)$ is the short-circuit current at solar

panel temperature 25°C , and the irradiation is $1\text{KW}/\text{m}^2$. The relationship exists between short-circuit current $I_{sc}(25^{\circ}\text{C}, 1\text{KW}/\text{m}^2)$ and photocurrent $I_{ph}(25^{\circ}\text{C}, 1\text{KW}/\text{m}^2)$ is expressed by using (12) at solar panel temperature 25°C , and the irradiation is $1\text{KW}/\text{m}^2$. The photocurrent I_{ph} is expressed by using (13) with the temperature and irradiation changing. Thus, using (6) and (13), the open-circuit voltage V_{oc} is evaluation. Thirdly, the diode factor n and reverse saturation current I_0 affect the output power. The n and I_0 are the unknown constant. Although different PVs have different n and I_0 , a piece of PV's n and I_0 is same. Normally, the n exists between 40 and 110, and the I_0 exists between $0.2\ \mu\text{A}$ and $500\ \mu\text{A}$. If the value of n and I_0 are known, the method is easy to acquire a piece of PV's maximum output power. The effect of n and I_0 are analysed in this paper. The irradiation S is expressed (14) as a function of I_{ph} .

2.2 Analyses of optimal output voltage V_{mppt}

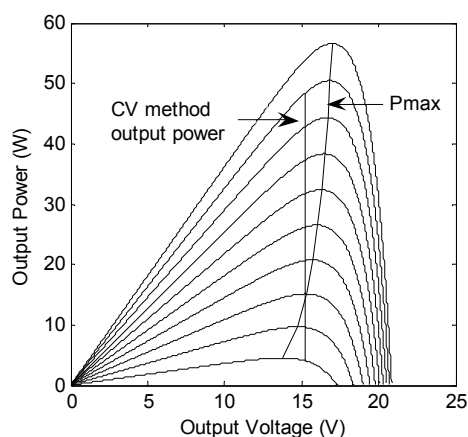


Fig.3 Draw a comparison between the output power of CV method and the actual P_{max} curve at temperature -20°C

For example, the open-circuit voltage V_{oc} and short-circuit current I_{sc} , which were measured at irradiation $1\text{KW}/\text{m}^2$ and temperature 25°C , are 22V and 3.8A , respectively. The changing coefficient K_i of I_{sc} and the changing coefficient K_v of V_{oc} were measured, are 0.001 and -0.004 , respectively. The diode factor n and reverse saturation current I_0 were supposed, are 60 and $5\ \mu\text{A}$, respectively. Fig. 2 shows P-V characteristics and P_{max} curve of PV are calculated using above values. Fig.2 (a) shows the maximum power curve at different temperature and same irradiation $800\text{W}/\text{m}^2$, Fig.2 (b) shows the maximum power curve at same temperature 45°C and different irradiation. It is confirmed through calculating results shown in Fig.2 that proportional

relationships between the open-circuit voltage and the optimal output voltage have been proposed in some literature. The proportionality coefficient using K , K is the coefficient of the optimum output voltage and the open-circuit voltage. K is expressed by using (15) at time n . In general, it is approximate equal 0.76 . Base on the conclusion, the maximum power point tracking is very easy under the known n and I_0 conditions.

$$V_{mppt}(n)/V_{oc}(n) = K \approx 0.76 \quad \square 15 \square$$

2.3 Analyses of maximum output power

The perturbation and observation (PO) method is well known as the hill-climbing method, it has been widely used because of its simple feedback structure and fewer measured parameters. But the PO method is not avoiding the power loss. The constant voltage (CV) method is very common, i.e. a cost-effective two-method MPPT control scheme is proposed in the literature [9] to track the maximum power point (MPP) at both low and high irradiation, by combining a Constant Voltage (CV) method and a modified PO algorithm. But the constant voltage (CV) method is impossible to exact acquire the maximum power (MP) point because of some problems is not be resolved, i.e., the efficiency is very low, and only one maximum power point (MPP) is tracked in the whole tracking course. Fig.3 shows the output power of CV method, and draws a comparison between the output power of CV method and the actual maximum power. As shown in Fig.3, only one maximum power point is tracked in the whole tracking course. As a conclusion, the CV method is impossible to exact track the MPP. The reason is not known the open-circuit voltage at that time. If the values of n and I_0 are known, the open-circuit voltage is easy gained by using (6). So the essential reason is not known the values of n and I_0 .

3 The proposed MPPT algorithms

Base on above data, n and I_0 were supposed, are 60 and $5\ \mu\text{A}$, respectively. The open-circuit voltage is easy gained. The optimal output voltage is gained at that time. As shown in Fig.4, the simulative and calculated results verified that the proposed method is more efficiency than the CV method. But Fig.4 shows an error exists between the actual maximum power curve and the power curve at $K=0.76$ under the known n and I_0 conditions. Fig. 4 (a) shows the P-I characteristics, and draws a comparison between the P_{max} curve and the P_{max}' curve at $K=0.76$ under same irradiation $600\text{W}/\text{m}^2$ and various temperature

conditions. Fig. 4 (b) shows the P-I characteristics, and draws a comparison between the P_{max} curve and the P_{max}' curve at $K=0.76$ under same temperature $-30^{\circ}C$ and various irradiation conditions. As shown in Fig.4, the coefficient K is not very accurate in the literature. The reason is not consider the effect of temperature and irradiation and diode factor n and reverse saturation current I_0 .

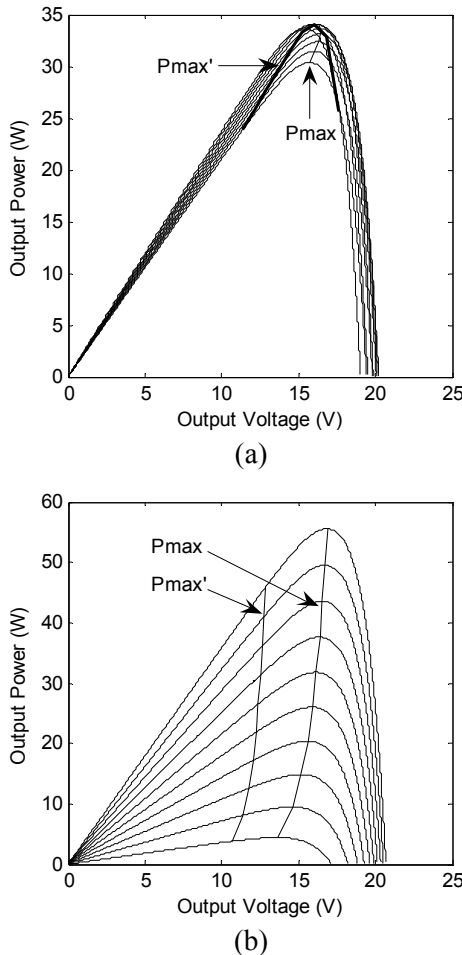


Fig.4 P-I characteristics, and draws a comparison between the P_{max} curve and the P_{max}' curve at $K=0.76$ under the known n and I_0 conditions. (a) The irradiation S is $600W/m^2$, and the temperature is changing from $-50^{\circ}C$ to $75^{\circ}C$. (b) The irradiation is changing from $100W/m^2$ to $1KW/m^2$ at the temperature $-30^{\circ}C$.

3.1 Relationship of n , I_0 and I_{ph}

As mention above, V_{oc} and I_{sc} , which were measured at irradiation $1KW/m^2$ and temperature $25^{\circ}C$, are $22V$ and $3.8A$, respectively. K_i and K_v were measured, are 0.001 and -0.004 , respectively. Fig. 5 shows P-I characteristics and P_{max} curve of PV, the data are calculated by using above values under the same n and different I_0 conditions. Fig.5 (a) shows the maximum power curve at same irradiation and

different temperature, Fig.5 (b) shows the maximum power curve at same temperature and different irradiation.

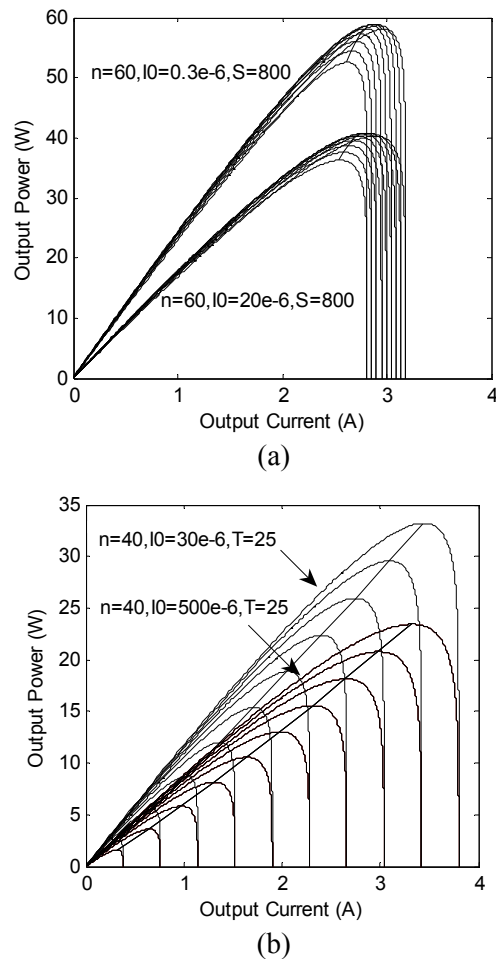
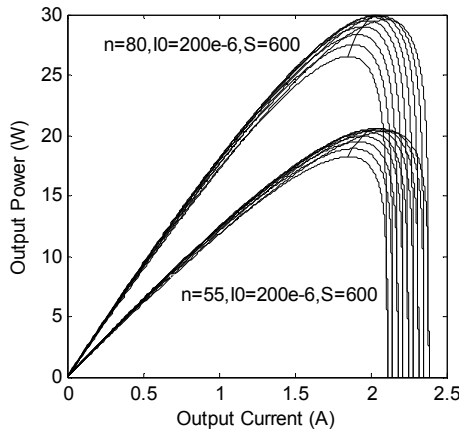
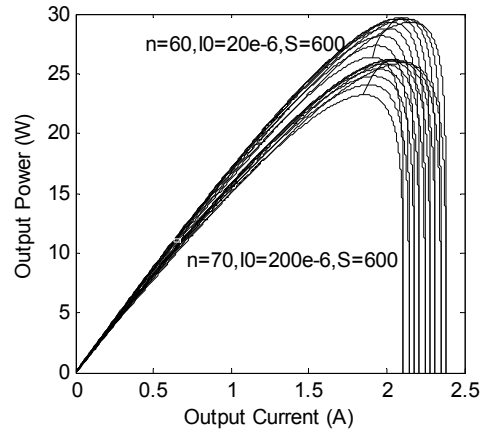


Fig.5 Calculated P-I characteristics and P_{max} curve under the same n and different I_0 conditions. (a) The irradiation S is $800W/m^2$, and the temperature is changing from $-50^{\circ}C$ to $75^{\circ}C$. (b) The irradiation is changing from $100W/m^2$ to $1KW/m^2$ at the temperature $25^{\circ}C$.

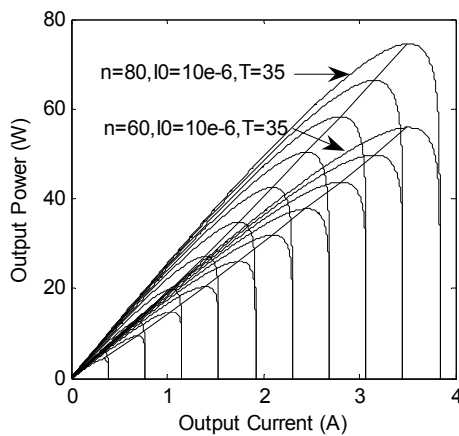
When the solar irradiation is steady, and the values is $800W/m^2$, and the temperature is changing from $-50^{\circ}C$ to $75^{\circ}C$, under same n and different I_0 conditions, Fig. 5 (a) shows that the photocurrent I_{ph} is same under same temperature conditions, and the output power is increasing with the I_0 decreasing from $500 \mu A$ to $0.2 \mu A$. When the temperature is steady and the values is $25^{\circ}C$, and the solar irradiation is changing from $100W/m^2$ to $1KW/m^2$ under same n and different I_0 conditions, Fig. 5 (b) shows that the photocurrent I_{ph} is same under same irradiation conditions, and the output power is increasing with the I_0 decreasing from $500 \mu A$ to $0.2 \mu A$.



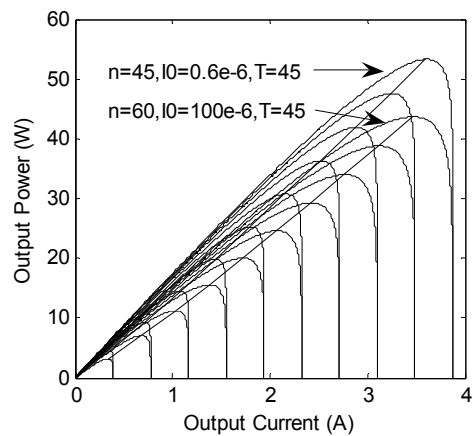
(a)



(a)



(b)



(b)

Fig.6 Calculated P-I characteristics and P_{max} curve under the different n and same I_0 conditions. (a) The irradiation S is $600W/m^2$, and the temperature is changing from $-50^{\circ}C$ to $75^{\circ}C$. (b) The irradiation is changing from $100W/m^2$ to $1KW/m^2$ at temperature $35^{\circ}C$.

If the weather conditions are same, Fig.7 shows that the output photocurrent I_{ph} is same under different n and different I_0 conditions. If the irradiation is $600W/m^2$, and the temperature is increasing from $-50^{\circ}C$ to $75^{\circ}C$, Fig. 7 (a) shows that the photocurrent I_{ph} is same under different diode factor n and different reverse saturation current I_0 conditions. If the temperature is $45^{\circ}C$, and the irradiation is increasing from $100W/m^2$ to $1KW/m^2$, Fig.7 (b) shows that the photocurrent I_{ph} is same under different diode factor n and different reverse saturation current I_0 conditions.

A conclusion is gained in this paper. If the weather conditions are same, the output photocurrent I_{ph} for a piece PV is same under different n and different I_0 conditions, and the conclusion is very important to acquire the maximum power point of PV system. Based on the conclusion, a novel method was presented to acquire the actual n and I_0 .

Fig.7 Calculated P-I characteristics and P_{max} curve under different n and I_0 . (a) If the irradiation S is $600W/m^2$, and the temperature is changing from $-50^{\circ}C$ to $75^{\circ}C$. (b) If the irradiation is changing from $100W/m^2$ to $1KW/m^2$ at $45^{\circ}C$.

3.2 Acquire the actual n and I_0

Firstly, the n and I_0 were supposed, are 40 and $500\mu A$, respectively. The output voltage V , the output current I and temperature T of PV is detected by using the Hall Effect sensors for current and voltage and temperature sensor, respectively. I_{ph} is given by using (5), and the assumptive maximum power point was gained. Fig.8 shows the assumptive maximum power point A of PV by using the assumptive n and I_0 under steady weather conditions. Secondly, Fig.8 shows the actual maximum power point B by using PO method at that time. The actual optimal output current $I_{m\ p\ p\ t}$ and optimal output voltage $V_{m\ p\ p\ t}$ is gained by using sensors. Based on above conclusion, the photocurrent I_{ph} is same under same weather conditions. The n is supposed minimum and the I_0 is supposed maximum. The actual maximum power point is more than the assumptive maximum power.

To gain the actual n and I_0 , the diode factor should increase and the reverse saturation current should decrease. According to the increasing values of diode factor and decreasing reverse saturation current I_0 , the photocurrent I_{ph} and actual optimal output current $I_{m_{ppt}}$ is used to calculate the assumptive optimal output voltage $V_{m_{ppt}1}$ by using (5). Then, the error between the actual optimal output voltage and assumptive optimal output voltage is ΔV , which can be expressed $V_{m_{ppt}1} - V_{m_{ppt}}$. Once $\Delta V = 0$, the diode factor n and reverse saturation current I_0 are actual value. Thus, the actual value of n and I_0 was saved, and PO method is stopped. Next, the process cited above is concretely explained by examples with number obtained based on Fig.8. First, the output voltage and output current were measured at time $n1$, are $7.0573V$ and $2.1812A$, respectively. In this case, the generated power $P(n1)$ is $15.3934W$. The temperature T of solar panel is $25^\circ C$ at time $n1$. Then, the diode factor n and reverse saturation current I_0 were supposed, are 40 and $500\mu A$, respectively. The photocurrent $I_{ph} = 2.66A$ is gained by using (5). The irradiation S is $700W/m^2$ by using (14). The temperature and irradiation are steady at enough long time. The calculated optimal output current and optimal output voltage were gained, are $2.3089A$ and $6.7400V$, respectively. The calculated optimal output power $P_{max}(n1)$ is $15.562W > P(n1)$. Second, the PO method is utilized to acquire the actual maximum power point under same weather conditions. The actual optimal output current $I_{m_{ppt}(n1)}$ and optimal output voltage $V_{m_{ppt}(n1)}$ were measured, are $2.3825A$ and $15.54V$, respectively. Thus, the maximum output power $P_{max}(n1)$ is $37.0245W$, and $(P_{max}(n1) > P_{max}'(n1))$. Based on above conclusion, in order to acquire the actual n and I_0 of a piece of PV it is obligatory to increase the diode factor n and decrease the reverse saturation current I_0 . In this case, the actual photocurrent I_{ph} and the optimal output current $I_{m_{ppt}(n1)}$ were used to calculate the assumptive optimal output voltage $V_{m_{ppt}1}$ by using (5). Then, the difference ΔV between the actual optimal output voltage and assumptive optimal output voltage is calculated. If $\Delta V = 0$, the actual value of the diode factor n and reverse saturation current I_0 is gained, are 70.2 and $50.45\mu A$, respectively. The values of actual n and I_0 were saved.

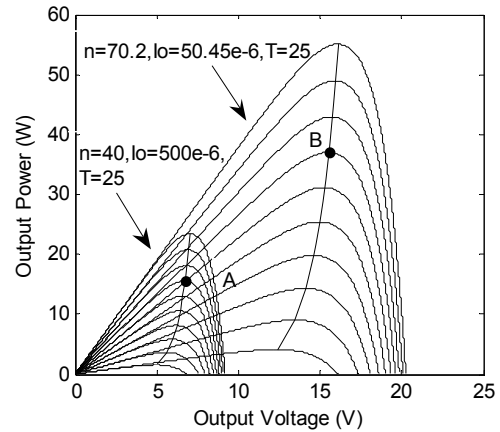


Fig.8 Calculated the actual diode factor n and reverse saturation current I_0 by using the combined perturb and observe (PO) method.

3.3 The proposed Variable Voltage MPPT algorithms

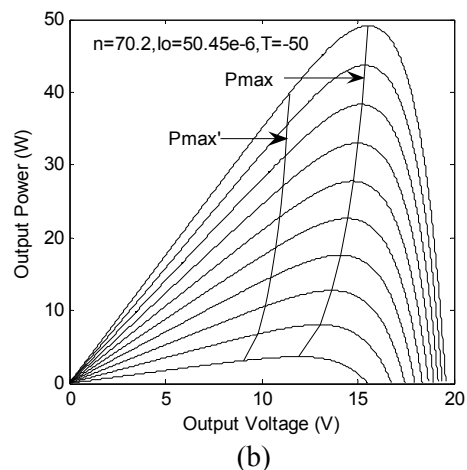
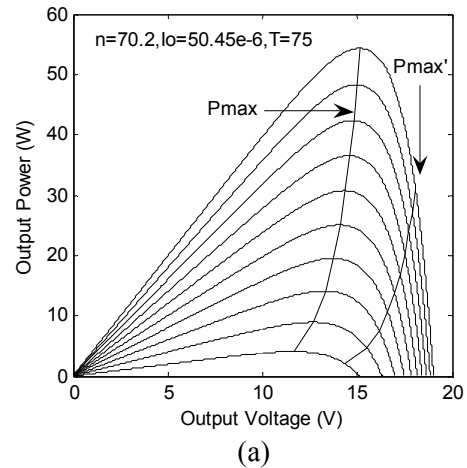
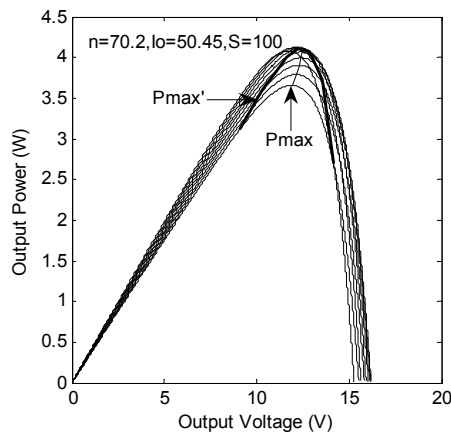


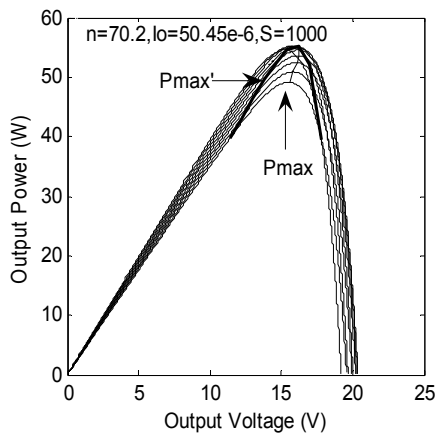
Fig.9 P_{max} curve and P_{max}' curve under different temperature conditions. (a) The irradiation is changing from $100W/m^2$ to $1KW/m^2$ at $75^\circ C$. (b) The irradiation is changing from $100W/m^2$ to $1KW/m^2$ at $-50^\circ C$.

As shown in Fig.4, an error exists between the

actual maximum power curve and the power curve at $K = 0.76$ under the known n and I_0 conditions. The reason is not consider the effect of temperature and irradiation and diode factor n and reverse saturation current I_0 . Theoretical and simulation results show that the effect of temperature and irradiation must be considered. The reverse saturation current I_0 has an important effect in order to acquire the actual K . The effect of diode factor n is very small. In order to acquire the actual K , the expiations of the temperature, irradiation and reverse saturation current I_0 are necessary.



(a)



(b)

Fig.10 P_{max} curve and P_{max}' curve under different irradiation conditions. (a) The irradiation S is $100W/m^2$, and the temperature is changing from $-50^\circ C$ to $75^\circ C$. (b) The irradiation S is $1000W/m^2$, and the temperature is changing from $-50^\circ C$ to $75^\circ C$.

According to above data, Fig.9 shows the actual maximum power P_{max} curve and the P_{max}' curve at $K = 0.76$ under different temperature conditions. The simulation results show that an error exists in two curves. As shown in Fig.9 (a), the actual optimal output voltage coefficient K is less than 0.76. Fig.9 (b) shows that the actual optimal output voltage

coefficient K is more than 0.76. In a word, the different temperatures have the different proportionality coefficient K . So the effect of temperature must be considered under different temperature in order to acquire the actual maximum power point. An expiation of temperature is necessary. Fig.10 shows the actual maximum power P_{max} curve and the P_{max}' curve at $K=0.76$ under different irradiation conditions. The simulation results show that an error exists in two curves.

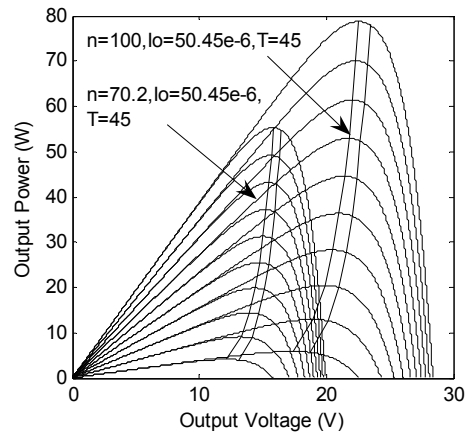


Fig.11 P_{max} curve and P_{max}' curve under different diode factor n conditions.

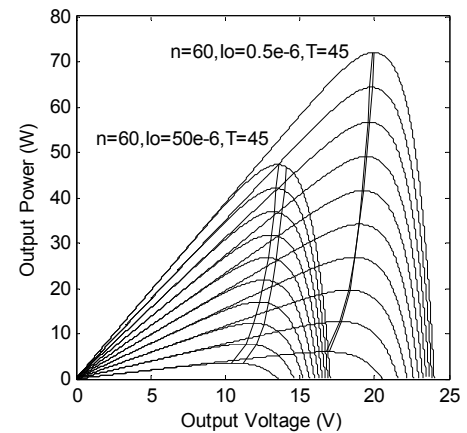


Fig.12 P_{max} curve and P_{max}' curve under different reverse saturation current I_0 conditions.

As shown in Fig.10, the effect is different under high irradiation or low irradiation conditions. The effect of irradiation must be thought under different irradiation conditions. An expiation of irradiation is necessary in order to gain the MPP. Fig.11 shows that the curves are approximate parallel under the different diode factor n conditions. The simulation results show the proportional relationships between the actual maximum power and the calculative output power is approximate equal. The effect of diode factor n is very small. An expiation of diode factor is not necessary. Fig.12 shows that the error between the P_{max} curve and the P_{max}' curve at $K = 0.76$ is different under different reverse saturation

current I_0 conditions. The effect of I_0 must be thought under different I_0 conditions. An expiation of I_0 is necessity.

Using (14), the irradiation can be gained at time m . Theoretical and simulation results show that the expiatory coefficient ΔK_s of irradiation is expressed (16) as a function of the irradiation S . The expiatory coefficient $\Delta 2$ is $0.000027m^2/W$ when the irradiation S is less than $750W/m^2$. Or else, the expiatory coefficient $\Delta 1$ is $0.000012m^2/W$. The expiatory coefficient ΔK_t of temperature is expressed (17) as a function of the temperature T_1 . The expiatory coefficient is a constant $0.0031/^{\circ}C$ under the temperature is less than $25^{\circ}C$. Or else, the expiatory coefficient is a constant $0.0033/^{\circ}C$. Here, T_1 is the actual solar panel temperature.

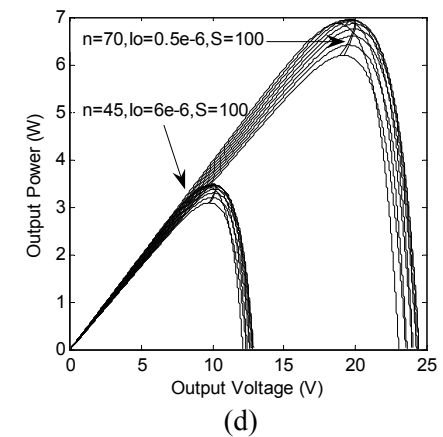
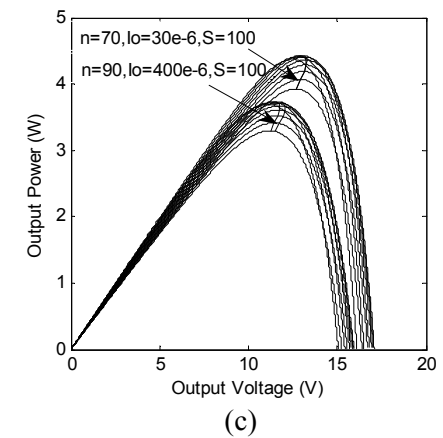
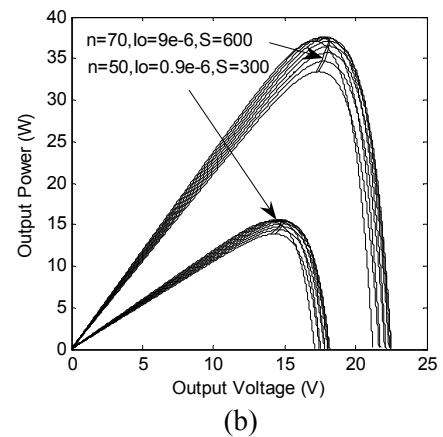
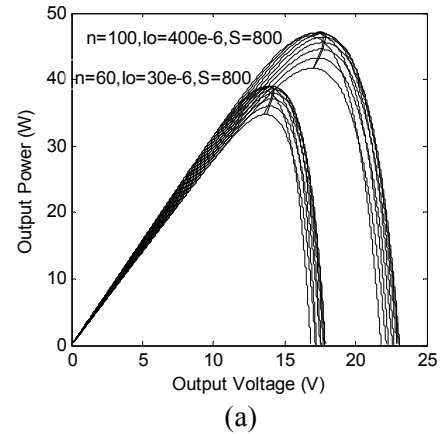
$$\Delta K_s = \begin{cases} (S - 750) \times \Delta 1 & S \geq 750W/m^2 \\ (S - 750) \times \Delta 2 & S < 750W/m^2 \end{cases} \quad (16)$$

$$\Delta K_t = \begin{cases} (T_1 - 25) \times 0.0031 & T_1 \leq 25^{\circ}C \\ (T_1 - 25) \times 0.0033 & T_1 > 25^{\circ}C \end{cases} \quad (17)$$

$$\Delta K_{I_0} = \begin{cases} 0.005 + 1e-4 \times \frac{((5e-4) - I_0)}{(5e-4)} \times 500 & I_0 \geq 400e-6 \\ 0.0149 & I_0 \geq 300e-6 \\ 0.005 + 5e-5 \times \frac{((5e-4) - I_0)}{(5e-4)} \times 500 & I_0 \geq 100e-6 \\ 0.033 + 5e-5 \times \frac{((1e-4) - I_0)}{(1e-4)} \times 100 & I_0 \geq 10e-6 \\ 0.05 + 0.002 \times \frac{((1e-5) - I_0)}{(1e-5)} \times 10 & I_0 \geq 1e-6 \\ 0.07 + 0.016 \times \frac{((1e-6) - I_0)}{(1e-6)} & I_0 > 0.2e-6 \end{cases} \quad (18)$$

$$Kp = 0.76 + \Delta K_s - \Delta K_t + \Delta K_{I_0} \quad (19)$$

The expiatory coefficient ΔK_{I_0} of reverse saturation current I_0 is expressed (18) as a function of I_0 . The expiatory coefficient is $1e-4/\mu A$ from 0.005 under the reverse saturation current I_0 is more than $0.4mA$ conditions. The expiatory coefficient is a constant $0.0149/\mu A$ under the I_0 more than $0.3mA$ and less than $0.4mA$ conditions. The expiatory coefficient is $5e-5/\mu A$ from 0.005 under the I_0 is more than $0.1mA$ and less than $0.3mA$ conditions. The expiatory coefficient is $5e-5/\mu A$ from 0.033 under the I_0 is more than $10\mu A$ and less than $0.1mA$ conditions. The expiatory coefficient is $0.002/\mu A$ from 0.05 under the I_0 is more than $1\mu A$ and less than $10\mu A$ conditions. Or else, the expiatory coefficient is $0.016/\mu A$ from 0.07 under the I_0 is more than $0.2\mu A$ and less than $1\mu A$ conditions.



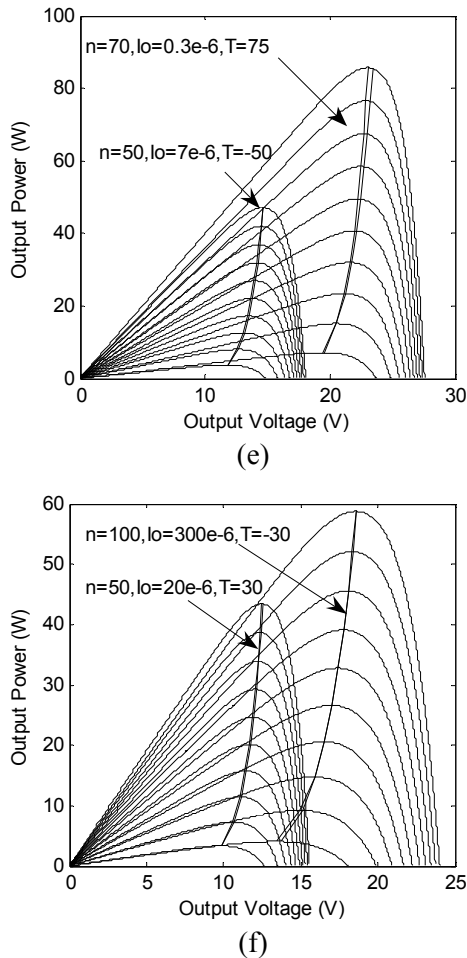


Fig.13 The P_{max} curve and P_{max}' curve are simulated under different n and different I_o conditions. (a)The I_o is more than $10 \mu A$. (b) The I_o is less than $10 \mu A$. (c) The I_o is more than $10 \mu A$, and the S less than $150 W/m^2$. (d) The I_o is less than $10 \mu A$, and the S less than $150 W/m^2$. (e) The I_o less than $10 \mu A$, and the n and T are different. (f) The I_o more than $10 \mu A$, and the n and T are different.

The integrated expiatory coefficient K_p is expressed (19). Fig.13 shows the simulation results under different n and different I_o conditions. As shown in Fig.13 (a), the expiatory coefficient is reasonable under the I_o is more than $10 \mu A$ conditions. Fig.13 (b) shows that the expiatory coefficient is reasonable under the I_o is less than $10 \mu A$ conditions. As shown in Fig.13 (c), the expiatory coefficient is reasonable under the I_o is more than $10 \mu A$ conditions at low irradiation. As shown in Fig.13 (d), the expiatory coefficient is reasonable under the I_o is less than $10 \mu A$ conditions at low irradiation. Fig.13 (e) shows that the expiation coefficient is reasonable under the I_o is less than $10 \mu A$ and different n and different T conditions. Fig.13 (f) shows that the expiatory coefficient is

reasonable under the I_o is more than $10 \mu A$ and different n and different T conditions.

Based on the results of Fig. 13, no matter how the solar radiation and solar panel temperature change, the maximum power point is gained by using the integrated expiatory coefficient K_p . The maximum power point is gained by using the integrated expiation coefficient K_p no matter how the values of n and I_o vary with various PV.

3.4 Flowchart of the proposed MPPT algorithm

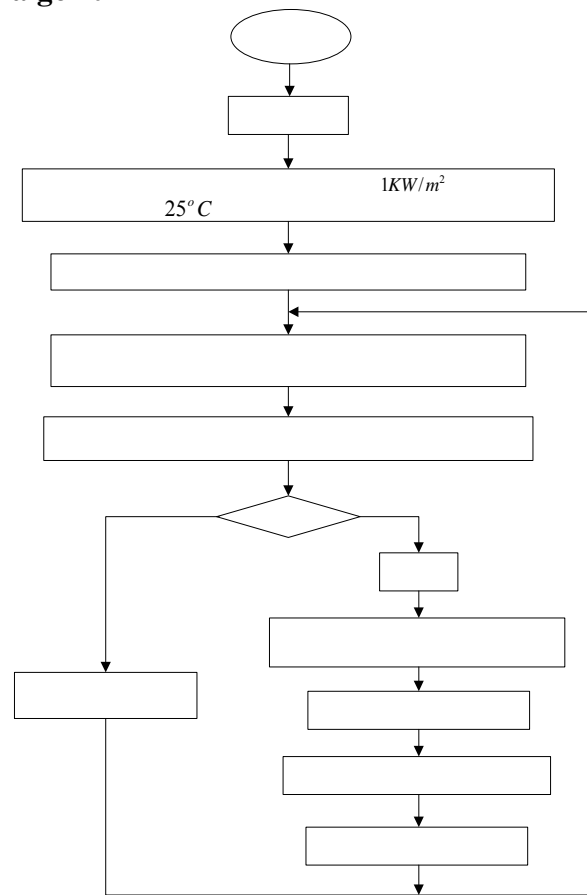


Fig.14 Flowchart of the proposed MPPT algorithm
The control procedure cited above is summarized in the flow chart shown in Fig.14. First, the open-circuit voltage V_{oc} and short-circuit current I_{sc} , which were measured at PV panel temperature $25^\circ C$ and high irradiation $1KW/m^2$, and m is defined zero. The changing coefficient K_i of I_{sc} and coefficient K_v of V_{oc} were measured, respectively. Second, The n and I_o are supposed at start-up state. Third, the output current $I(n)$ and the output voltage $V(n)$ and the temperature T were detected by using sensors at time $n1$. Then, the photocurrent $I_{ph}(n1)$ and the irradiation $S(n1)$ and the open-circuit voltage

$V_{oc}(n)$ were calculated by using the supposed n and I_o . Next, the expiatory program of reference voltage is applied in order to acquire the supposed maximum power P_{max} . Compare m with 10, and if the value of m is less than 10, the value of m adds one. The actual maximum power point is gained by using the PO method under same weather conditions. The actual values of n and I_o are gained, and the values are saved, and the average values is calculated. Or else, the actual values of n and I_o were applied to acquire the maximum power P_{max} at the time, and then the PO method is stopped. The proposed MPPT algorithm is high efficiency to track the maximum output power of PV compare with the conventional CV method.

4 Verification of the proposed MPPT algorithm

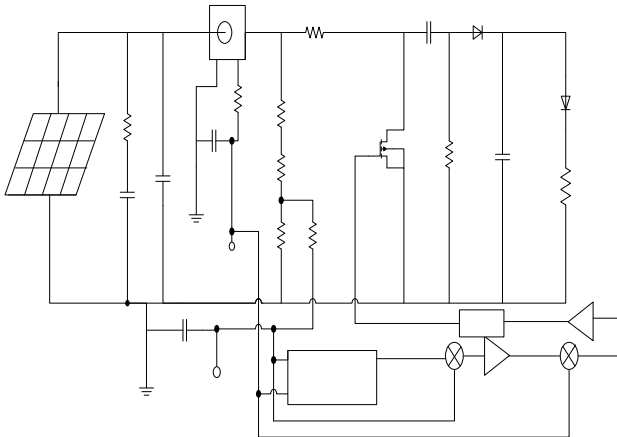
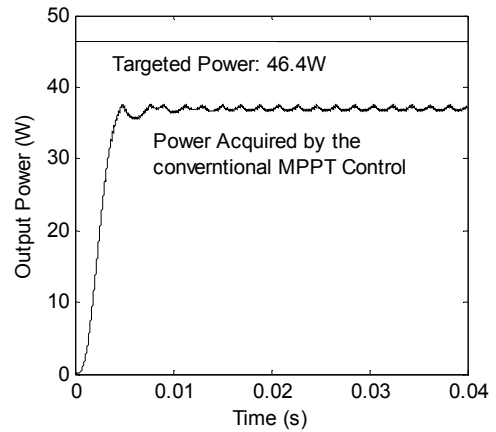


Fig.15 Block diagram of series-connected load control for PV generation systems.

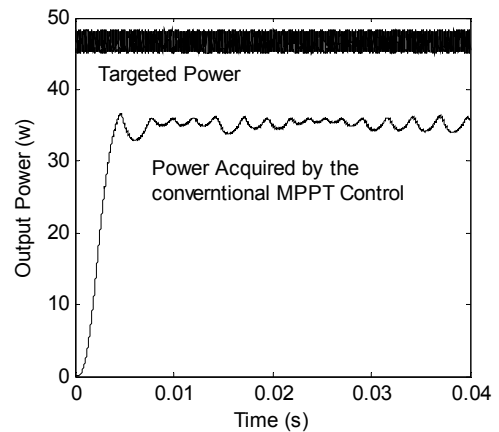
Fig.15 shows the block diagram of load control. The classical Sepic converter is used to track the maximum power point. It consists of two inductances, two capacitors, one diode, one MOSFET, the input PV and the load resistance at the output of the circuit [14]. The advantages of Sepic converter include the continuous input current and wide output voltage range. Additionally, not only it can provide isolation between the DC input and the DC load, but also it can reduce the reverse-recovery loss and improve the power efficiency [15]. Compared the conventional Buck or Boost converters, it allows a low current ripple under low level DC voltage conditions [16].

The MOSFET switch is controlled by a multiple-loop control scheme in order to acquire the maximum power point of PV. The multiple-loop control scheme can ensure a line current wave-shaping and an appropriate DC voltage. A conventional method is used in the paper. The

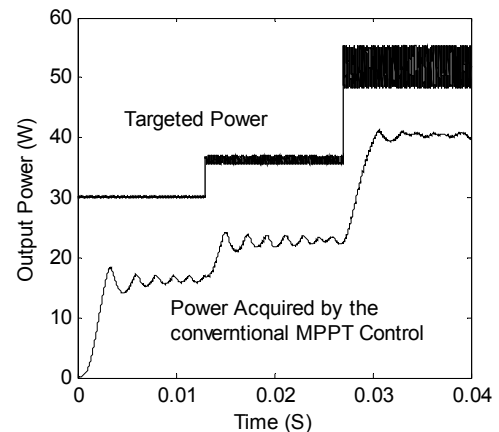
current-loop is used to inner-loop, and the voltage-loop is used to outer-loop. The optimal output voltage is calculated to act as the reference input by using DSP. The PI controller is used to improve the input performance of PWM. The output of PWM is used to control the switch frequency of MOSFET. The control scheme is very easy to track the maximum power point under various weather conditions, which is described to compare with the proposed control method in next section.



(a)



(b)



(c)

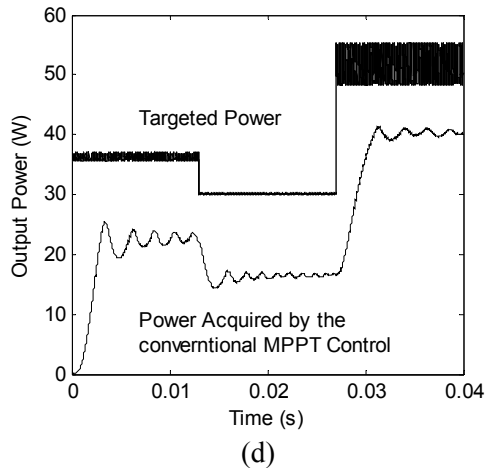


Fig.16 The conventional control scheme is responded under various load resistance conditions. (a) The irradiation is fixed. (b) The disturbed signals exist. (c)The irradiation is gradual increasing. (d)The irradiation is wavy.

If the load resistance is various, Fig.16 (a) shows that the conventional control scheme can not track the power very well under the fixed irradiation conditions. Fig.16 (b) shows that the conventional control scheme is not very feasible under the fixed irradiation have the disturbed signals conditions. Fig.16 (c) shows that the conventional control scheme is relatively low conversion efficiency under the gradual increasing irradiation have the disturbed signals conditions. As shown in the Fig.16 (d), the efficiency is low at wavy irradiation. Based on the results of Fig.16, no matter how the disturbed signals are various with the time, the output efficiency of conventional MPPT control scheme is not more than 85% under different load resistance conditions.

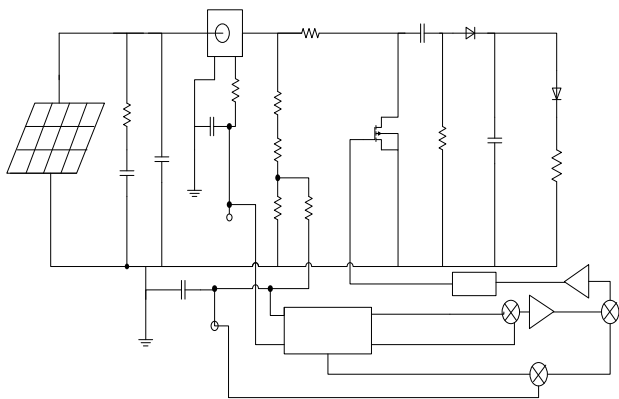
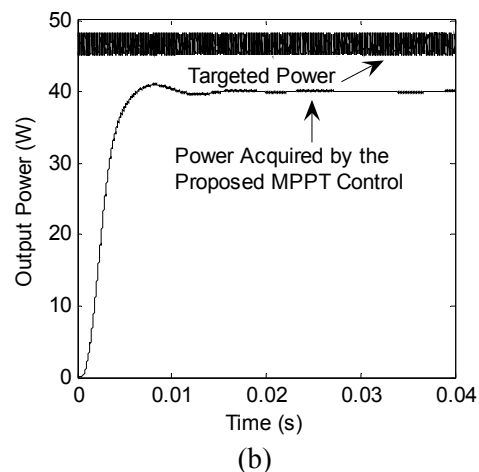
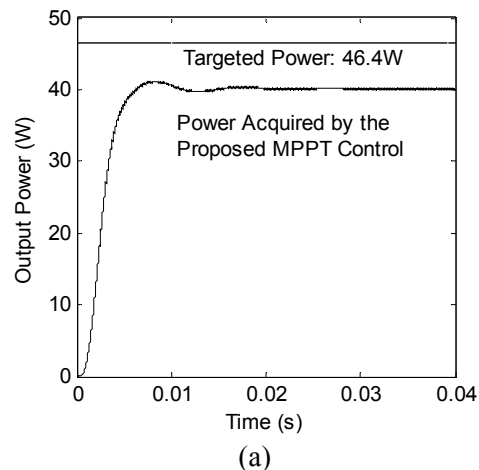


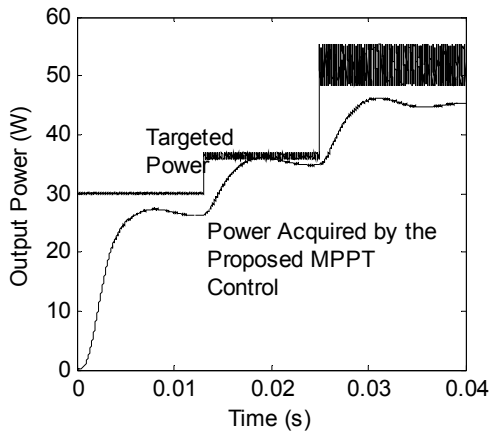
Fig.17 Improved block diagram of series-connected load control for PV generation systems.

As shown in the Fig.17, a proposed control scheme is described in the paper. An easy improvement is described in order to acquire the higher efficiency than the conventional control method. The voltage-loop is used to inner-loop, and the power-loop is used to outer-loop. The maximum

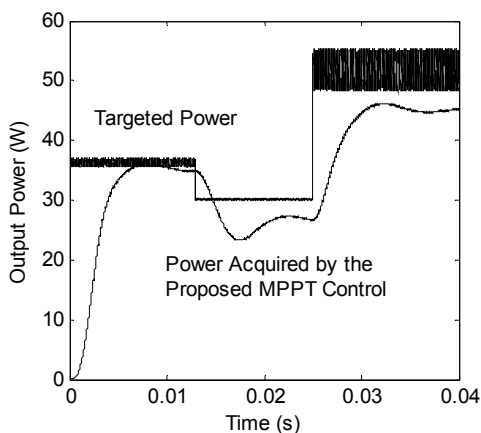
output power and the optimal output voltage are calculated to act as the reference input of control.

Fig.18 shows that the proposed control scheme is responded under different irradiation and resistances conditions. Fig.18 (a) shown that the proposed control scheme can track the power very well under the fixed irradiation conditions. Fig.18 (b) shows that the proposed control scheme is very feasible under the fixed irradiation have the disturbed signals conditions. As shown in Fig.18 (c), the output power of PV is increasing with the increase of irradiation. Not matter how the disturbed signals are various with time, the proposed MPPT control scheme can track the targeted power which is calculated by using DSP and the proposed MPPT algorithm. Fig.18 (d) show that the output power is various with the different of irradiation under evil weather conditions. Base on the results of Fig.18, the proposed MPPT algorithm is very easy to rapid calculate the maximum power point under smart various weather conditions. Base on the known n and I_o , the maximum power algorithm is very rapid to acquire the maximum power point in the whole tracking course by using the proposed Sepic circuit.





(c)



(d)

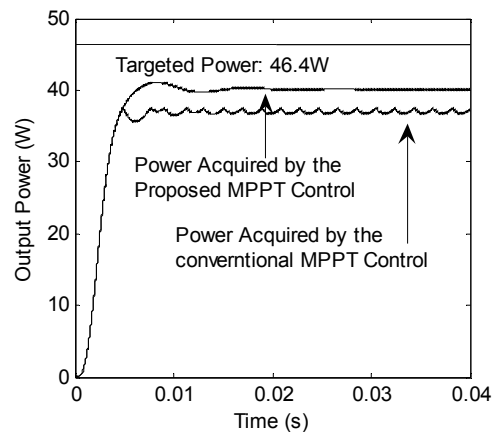
Fig.18 The proposed control scheme is responded under various irradiation and the disturbed signals exist conditions. (a) The irradiation is fixed. (b) The disturbed signals exist. (c) The irradiation is increasing with the time. (d) The irradiation is wavy.

As shown in the Fig.19, the proposed control scheme is compared with the conventional control method under different irradiation conditions. Fig.19 (a) shows that the output efficiency of proposed MPPT control scheme is more than the conventional control scheme under different load resistance and fixed irradiation conditions. Fig.19 (b) shows that the output efficiency of proposed MPPT control scheme under the fixed irradiation has the disturbed signals conditions. As shown in the Fig.19 (c), the output efficiency of proposed MPPT control scheme is more than the conventional control scheme under the gradual increasing irradiation has the disturbed signals conditions. The same conclusion can be gained from the Fig.19 (d) under the wavy irradiation conditions.

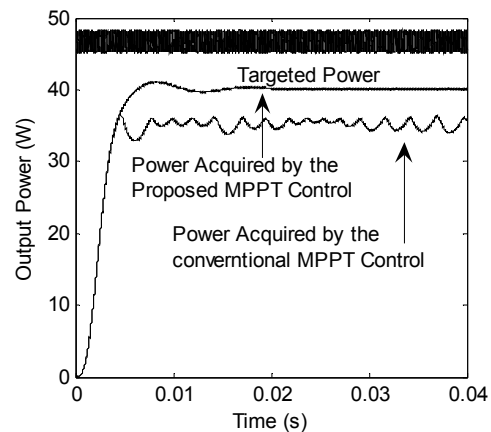
As shown in the Fig.19, the proposed MPPT algorithm is very easy to rapid calculate the maximum power point under smart various weather conditions. The proposed control scheme has higher

output efficiency than the conventional control scheme. So the proposed variable voltage MPPT control method can acquire maximum available power from PV generation system with the changing of ambient weather at real time. The proposed double loop control improves the output efficiency of traditional control method. It is evident that the PV generation system with variable voltage MPPT algorithm has a good dynamic performance duo to the actual n and I_o is gained.

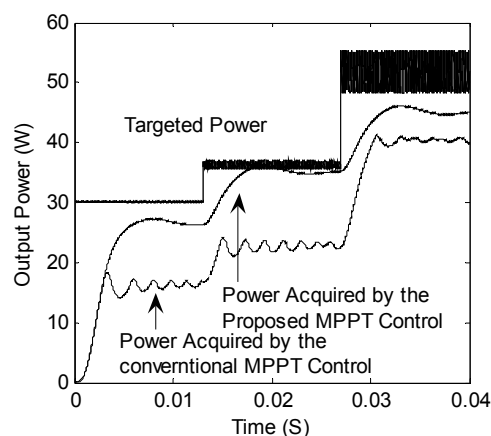
Certainly, the aging and partial shading will change the output characteristic of actual PV system, so it is essential to run the PO method to gain the new actual n and I_o when the PV have been used a period of time. The variable step size PO method should be used to gain accurate n and I_o . And the incremental conductance (IC) method can be used to gain the actual n and I_o by introducing the method in above section under steady weather conditions. In the future, the intelligent theory should be used to improve PI characteristic of control scheme, i.e., the fuzzy theory, the immune theory, and the nerve net theory etc. And the intelligent MPPT control method is expected to improve the output efficiency of PV compare with traditional control method.



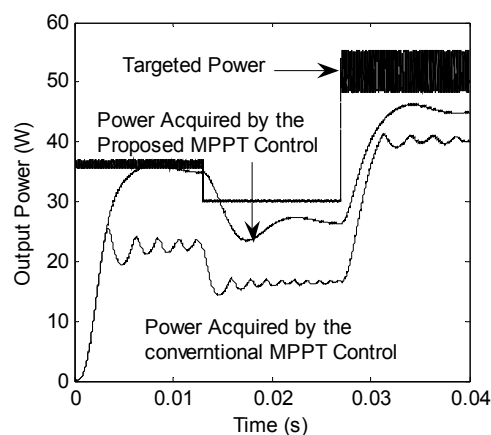
(a)



(b)



(c)



(d)

Fig.19 Draw a comparison between the proposed control scheme and the conventional control method under different irradiation conditions. (a) The irradiation is fixed. (b) The disturbed signals exist. (c) The irradiation is increasing with the time. (d) The irradiation is wavy.

5 Conclusion

A novel MPPT control method was proposed in this paper. A new method of acquire the actual n and I_o are proposed by using the PO method. The expiatory program of reference voltage is applied to acquire the actual maximum power point. The correctness and validity of expiatory coefficients is verified through simulation under various weather conditions. In order to acquire the maximum power, the PO method is applied to acquire the actual n and I_o , but it is not applied to acquire the MPP during tracking course, the loss of energy of PV is very small, and the output efficiency of proposed MPPT algorithm is more than 99%. Next, the proposed PI control scheme of MPPT and the Sepic circuit are used to track the maximum power point by controlling the switch frequency of MOSFET. The

proposed control scheme has move efficiency than the conventional control scheme.

ACKNOWLEDGMENT

THIS PROJECT WAS GRANTED FINANCIAL SUPPORT FROM CHINESE POSTDOCTORAL RESEARCH FOUNDATION (NO: 08R214134), SHANGHAI BAI YU LAN SCIENCE AND TECHONLGY FOUNDATION (NO: 2007B073), AND CHINA EDUCATION MINISTRY RESEARCH FOUNDATION (NO: 20071108), SCIENCE RESEARCH AND DEVELOPMENT PROGRAM OF SHANXI PROVINCE (NO: 200811026), YOUTH SCIENCE RESEARCH FOUNDATION OF SHANXI PROVINCE (NO: 2009021020).

References:

- [1] Yang Chen, Keyue Ma Smedley. A Cost-Effective Single-Stage Inverter with Maximum Power Point Tracking. *IEEE Transactions on Power Electronics*, 2004, 19(5): 1289–1294.
- [2] Mutoh, N, Inoue, T. A controlling method for charging photovoltaic generation power obtained by a MPPT control method to series connected ultraelectric double layer capacitors. In: *Industry Applications Conference, 39th IAS Annual Meeting, Conference Record of the 2004 IEEE*. 4: 2264 – 2271.
- [3] N. Mutoh, M. Ohno, T. Inoue. A Method for MPPT Control While Searching for Parameters Corresponding to Weather Conditions for PV Generate Systems. *Industrial Electronics, IEEE Transactions*, 2006, 53(4):1055-1065.
- [4] N. Mutoh, M. Ohno, T. Inoue. A Control Method to Charge Series-Connected Ultraelectric Double-Layer Capacitors Suitable for Photovoltaic Generate Systems Combining MPPT Control Method. *IEEE Transactions on Industrial Electronics*, 2007, 54(1): 374-383.
- [5] Arias, J, Linera, F.F, Martin-Ramos, J, Pernia, A.M, Cambronero, J. A modular PV regulator based on microcontroller with maximum power point tracking. *Industry Applications, 39th IAS Annual Meeting, Conference Record of IEEE*, 2004, 2: 1178–1184.
- [6] K. K. Tse, Billy M. T. Ho, Henry Shu-Hung Chung. A Comparative Study of Maximum-Power-Point Trackers for Photovoltaic Panels Using Switching-Frequency Modulation Scheme. *IEEE Transactions on Industrial Electronics*, 2004, 51(2): 410-418.
- [7] Peter Wolfs, Quan Li. A Current-Sensor-Free Incremental Conductance Single Cell MPPT for

- High Performance Vehicle Solar Arrays. In: Power Electronics Specialists Conference PESC '06, 37th IEEE, 2006: 1–7.
- [8] W.J.A.Teulings, J.C.Marpinard, A.Capel, D.O' Sullivan. A new maximum power point tracking system. In: Power Electronics Specialists Conference PESC '93 Record, 24th Annual IEEE, 1993: 833–838.
- [9] C. Dorofte, U. Borup, F. Blaabjerg. A combined two-method MPPT control scheme for grid-connected photovoltaic systems. In: Power Electronics and Applications, European Conference, 2005: 1-10.
- [10] M. Godoy Simoes, N. N. Franceschetti, M. Friedhofer. A fuzzy logic based photovoltaic peak power tracking controller. In: Industrial Electronics Proceedings ISIE '98, IEEE International Symposium 1: 300–305.
- [11] Tsai-Fu Wu, Chien-Hsuan Chang, Yu-Kai Chen. A fuzzy-logic-controlled single-stage converter for PV-powered lighting systems applications. IEEE Trans. Ind. Electron, 2000, 47(2): 287–296.
- [12] Ji, Changan, Zhang, Xiubin, Zeng, Guohui, He, Bin, Zhou, Xuelian, The study of the application based on fuzzy control for hybrid photovoltaic-wind renewable energy sources . WSEAS Transactions on Circuits and Systems, Vol.5, NO.1, January, 2006, pp. 9-16.
- [13] Liu, Li-qun, Wang Zhi-xin, A Rapid MPPT Algorithm Based on the Research of Solar Cell's Diode Factor and Reverse Saturation Current. WSEAS Transactions on Systems, 2008, 7(5):568-579.
- [14] A. Hren; P. Slibar, Full order dynamic model of SEPIC converter. Industrial Electronics, ISIE 2005. Proceedings of the IEEE International Symposium, 2005 (2):553–558.
- [15] J.-M. Kwon, W.-Y. Choi, J.-J. Lee, E.-H. Kim, B.-H. Kwon, Continuous-conduction-mode SEPIC converter with low reverse-recovery loss for power factor correction, Electric Power Applications, IEE Proceedings, 2006, 153(5):673-681.
- [16] H.Y. Kanaan, K. Al-Haddad , F. Fnaiech, Switching-function-based modeling and control of a SEPIC power factor correction circuit operating in continuous and discontinuous current modes, Industrial Technology, IEEE ICIT '04. 2004, 1:431–437.